In revision:
Neuroreport

Propagating wave activity in a tangential cortical slice

Charles C. Lee

Department of Comparative Biomedical Sciences, LSU School of Veterinary Medicine, Baton Rouge, LA 70803

Number of text pages: 11
Number of Figures: 3
Number of Supplementary Movies: 2

Running title: Tangential cortical slice

Correspondence to: Charles C. Lee
Department of Comparative Biomedical Sciences
LSU School of Veterinary Medicine
Baton Rouge, LA 70803

Email: cclee@lsu.edu

ABSTRACT

Propagating neural waves in the cerebral cortex influence the integration of incoming sensory information with ongoing cortical activity. However, the neural circuit elements that support these cortical waves remain to be fully defined. Here, a novel tangential slice preparation was developed that exhibited propagating wave activity across the dorsal cortical sheet, as assessed using autofluorescence imaging following focal electrical stimulation. Analysis of functional connectivity in the slice preparation with laser-scanning photostimulation via glutamate uncaging (LSPS) revealed a lack of short-latency, presumed monosynaptic, long-range connections (>300 μm) in the slice preparation. These results establish a novel slice preparation for assessing cortical dynamics and support the proposition that interactions among local cortical elements are sufficient to enable widespread propagating wave activity.

INTRODUCTION

The propagation of neural activity in the cerebral cortex utilizes both local and long-range connections among cortical areas [1-6]. In this manner, information is communicated among different cortical regions to integrate incoming sensory streams with ongoing network activity [4, 7-10]. The propagation of such activity across the cortical surface relies on both the network architecture and the balance of excitatory and inhibitory inputs [1, 7, 11, 12]. However, the degree to which local and long-range connections support such propagating cortical wave activity remains to be fully defined [7]. Determining the necessary and sufficient elements that support such activity would benefit from preparations that isolate the individual network components [13, 14].

As an approach to characterizing such propagating wave activity, a novel *in vitro* slice preparation of the neocortex in the mouse was developed that preserved much of the rostrocaudal and mediolateral extents of the dorsal cortical surface, primarily encompassing sensory and motor areas [15]. Although prior *in vivo* studies have observed propagating waves in these regions, connections to subcortical sites potentially complicates their interpretation [1-12]. Similarly, prior *in vitro* analyses of tangential cortical activity have typically been confined to more limited cortical domains, potentially constraining wave

dynamics [13, 14, 16]. Utilizing this novel *in vitro* slice preparation enabled the broad assessment of spatial and temporal patterns of activity following network perturbation, with prominent cortical wave activity observed using flavoprotein autofluorescence imaging [17-19]. In addition, laser-scanning photostimulation via uncaging of glutamate (LSPS) was employed to probe functional connectivity in the tangential cortical slice preparation [20-22].

From these studies, widespread but variable patterns of cortical wave activity were observed in this tangential slice preparation, but few long-range monosynaptic inputs to single neurons were detected with LSPS mapping. As such, these data support the notion that local connectivity may be sufficient to propagate wave activity across the cortical surface and influence computational processes on a global scale.

MATERIALS AND METHODS

Acute brain slices were prepared from C57BL/6J mice. All procedures were approved by the Institutional Animal Care and Use Committee (IACUC) of the Louisiana State University School of Veterinary Medicine. Animals were deeply anesthetized via inhalation of isoflurane. The brains were quickly removed and submerged in cool, oxygenated (95% O_2-5% CO_2), artificial cerebral spinal fluid (ACSF; in mM: 125 NaCl, 25 $NaHCO_3$, 3 KCl, 1.25 NaH_2PO_4, 1 $MgCl_2$, 2 $CaCl_2$, 25 glucose) and then blocked by tipping the brain by 10^o and fixing the ventral surface to tangentially approach the naturally flattened dorsal cerebrum of the mouse (Fig. 1C, inset). The cutting blade was then lowered towards the dorsal cerebral surface and vibratome sectioned dorsoventrally at 500 μm. The slices collected thus capture many of the dorsal cortical areas of the mouse, e.g.. visual, somatosensory, motor, and prefrontal (Fig. 1). Slices were then incubated at 32^{o}C in ACSF for 1 h.

For physiological recordings, the second section collected, representing ~250-750 μm below the pial surface, was transferred to a submerged perfusion chamber (Automate Scientific, Berkeley, CA) mounted on a custom microscope stage (Siskiyou, Grants Pass, OR) perfused continuously with oxygenated (95% O_2-5% CO_2), ACSF at 32^{o}C, warmed with an in-line solution heater (Warner Instruments, Hamden, CT), at a rate of 2-5 ml/min, supplied with a peristaltic perfusion pump (World Precision Instruments,

Sarasota, FL). Oxygenation and inclusion of glucose in the ACSF was necessary to observe the wave activity. Whole-cell recordings were made using a patch pipette filled with a cesium intracellular solution (in mM: 110 mM d-gluconic acid, 110 mM CsOH, 10 mM CsCl2, 1 mM CaCl2, 1 mM EGTA, 1 mM Mg-ATP, 10 mM HEPES, pH 7.3 obtained with KOH and osmolality of 290 mOsm obtained with distilled water). Biocytin was not included in the recording pipette, due to ambiguity of assessing recovered cell morphologies in the tangential slice plane, which necessarily truncates their apical and basal dendrites (see Discussion). —Voltage clamp recordings were made using a Multiclamp 700B amplifier and pCLAMP software (Molecular Devices, Sunnyvale, CA) and Ephus software (Janelia Farms, Ashburn, VA) [23].

Metabolic activity in response to electrical stimulation was measured by capturing green light (~510–540 nm) generated by mitochondrial flavoproteins in the presence of blue light (~450–490 nm) using epifluorescent illumination with a GFP filter cube set (Edmund Optics, Barrington, NJ) and a high-sensitivity camera, Q-Retiga SRV (Qimaging, Surrey, BC) [17-19]. In order to preserve optical clarity with the slice, electrical stimulation was performed using a glass pipette electrode filled with ACSF. The stimulating electrode was situated in the center of the slice preparation to deliver a short pulse train. Stimulation parameters were set at 125 Hz for 800 ms; 40-150 μA, based on prior experiments that demonstrated these as optimal for eliciting flavoprotein responses in slice preparations [19, 24]. Optical recordings were taken over 12 s using StreamPix software (NorPix, Montreal, Quebec), with an image exposure time ranging from 80 to 150 ms. Images were collected using an Olympus BX-51 microscope mounted with a UPlanSApo 4X, NA0.16, WD13mm, infinity corrected objective (Olympus America, Center Valley, PA). The images were processed using custom software running on Matlab (MathWorks, Nartick, MA) and the signal profiles were analyzed using ImageJ (NIH, Bethesda, MD) [19, 25].

Laser-scanning photostimulation (LSPS) with caged glutamate was used to map the cortical regions eliciting EPSP/Cs in recorded neurons, as previously described [20-22]. Nitroindolinyl (NI)-caged glutamate (0.37 mM; Sigma-RBI) was added to the recirculating ACSF. Photolysis of the caged glutamate was done focally with a pulsed UV laser (DPSS Lasers, Santa Clara, CA), with power adjusted between 5-50 mW with a variable neutral density wheel (Edmund Optics, Barrington, NJ). Custom software (Ephus)

written in MATLAB was used to analyze the data [23]. The evoked postsynaptic currents were superimposed on photomicrographs corresponding to the stimulation sites and mean responses plotted using Ephus.

For histological analysis, VGAT-Venus transgenic mice (colony established courtesy of Dr. Janice Naegele at Wesleyan University) were employed to aid in the assessment of inhibitory neuronal distribution in the tangential slice plane [21, 26-28]. Animals were deeply anesthetized with isoflurane and sacrificed via transcardiac perfusion, using 10 mM phosphate-buffered saline (PBS) solution, followed by 4% paraformaldehyde (PFA) in 10 mM PBS fixative. The brain was then removed and postfixed in 4% PFA in 10 mM PBS at 4° C for 24 hours, after which it was stored in a 4% PFA with 30% sucrose solution in 10 mM PBS for 24 hours for cryoprotection at 4° C. Subsequently, the brain was cryosectioned and the sections mounted and coverslipped on slides using Vectashield anti-fade mounting medium containing DAPI and Phalloidin (Vector Labs, Burlingame, CA). Images were collected using an FM-820T epifluorescence microscope (Amscope, Irvine, CA) and analyzed using ImageJ (NIH, Bethesda, MD).

RESULTS

A novel *in vitro* tangential slice preparation of the dorsal cerebrum in the mouse was prepared that contained intact functional neuronal connections, primarily among middle cortical layers, from ~250-750 μm below the pial surface (Fig. 1). The preparation preserved much of the dorsal cortical surface of the mouse brain, spanning roughly 9 mm rostrocaudally and 5 mm lateromedially, along their longest respective axes and encompassed most of the dorsal sensory, motor, and prefrontal areas (Fig. 1A) [15] . The cytoarchitectural organization of the slice preparation was examined in the VGAT-Venus transgenic mouse strain, which expresses the Venus fluorescent protein in inhibitory neurons (Fig. 1B). The distribution of inhibitory neurons varied across the tangential slice surface, being relatively more concentrated in the central than peripheral regions of the slice preparation, as seen in the variable concentrations of Venus expressing cells across the surface (Fig. 1B). Similarly varied distributions of

fiber and cell bodies were observed across the slice that correlated with the Venus labeling, as assessed by co-staining with DAPI and Phalloidin, respectively (Fig. 1C, D).

In order to assess patterns of cortical activity, flavoprotein autofluorescence imaging of the slice preparation was analyzed following focal electrical stimulation (Fig. 2). This imaging modality enables the assessment of broad patterns of cortical activity by measuring changes in mitochondrial flavoprotein autofluorescence that accompanies the increased metabolic demands of activated neurons and glia, as discussed below [17]. Following electrical stimulation, propagating waves of neuronal activity were observed across the cortical surface, which generally settled into local attractors, or functional sinks, at single or multiple cortical foci that persisted for several seconds following stimulation (Fig. 2A-D; Supplementary Movies). In general, two broad patterns of activity were observed that were classified as divergent (Fig. 2A-B; Supplementary Movie 1) or convergent (Fig. 2C-D; Supplementary Movie 2). The divergent activity pattern initiated at a single locus and spread to multiple distant loci (Fig. 2A-B; Supplementary Movie 1), while the convergent pattern initiated at the periphery before coalescing into a central locus of activity (Fig. 2C-D; Supplementary Movie 2).

The structural basis supporting these propagating waves was assessed by mapping functional connectivity in the slice using laser-scanning photostimulation via glutamate uncaging [20]. Whole-cell, voltage clamp recordings were made from neurons in the central region of the slice preparation and the elicited postsynaptic currents (PSCs) assessed from a 16 X 16 photostimulation grid, with 80 μm spacing between stimulation sites (Fig. 3A). Both evoked excitatory (EPSCs) and inhibitory (IPSCs) postsynaptic currents were elicited following photostimulation, while holding the cell at -20 mV. IPSCs dominated close to the recording site (<~200 μm), while weaker, longer-latency, EPSCs were observed outside of this domain (Fig. 3A). No short latency (<10 ms) responses were observed outside ~300 μm of the recording site, while some long latency, presumed polysynaptic, responses were found within ~400 μm (Fig. 3A-C), even at low laser stimulation power. These data suggest that functional connections in this tangential slice preparation are restricted to short-range local connections within ~300 μm.

DISCUSSION

In this study, a novel *in vitro* tangential slice preparation was developed that exhibited diverse patterns of propagating wave activity, with intact, local (<300 μm), neural circuit connections. These results support the proposition that functionally coupled local circuits are sufficient to enable the propagation of wave activity across the cortical surface [6, 7, 10, 12]. Although this tangential slice preparation exhibited cytoarchitectural variation across the surface, the diversity of cortical activity observed may result from such variable preservation of interlaminar architectures. Moreover, the apical and basal dendrites of preserved neurons are truncated in this slice plane, consequently affecting the preserved synaptic connections. The resultant network architecture may favor the polysynaptic activity necessary for propagating cortical waves, but which may technically limit its utility and relevance to fully intact cortical structures ~~, which could yield divergent attractor networks functionally coupled to *in vivo* processing states~~ [1-12]. In this regard, short-range cortical connections may be sufficiently robust and degenerate to usurp the laminar and dendritic variability across the tangential slice surface [29].

The assessment here of propagating wave activity with autofluorescence imaging contrasts with prior approaches that utilized other imaging and electrophysiological methods to characterize these waves [4, 9, 13, 14, 29-31]. Although autofluorescence imaging correlates with neural activity, it is an indirect measure that differs in its time course [17, 25]. Nevertheless, this imaging approach is highly sensitive, since electrophysiologically measured neural activity correlates absolutely with the autofluorecence signal [24, 32]. Interestingly, the source of the autofluorescence signal remains somewhat open, although most likely reflects mitochondrial activation at presynaptic and/or postsynaptic terminals. In addition, the broad spatiotemporal profile of the autofluorescence signal has been shown to reflect both monosynaptic and polysynaptic activation, which can reflect differences in synaptic strength, composition, and integrity [17, 24, 32]. Thus, the spatial activation patterns observed here likely corresponds directly with those predicted for electrophysiological measurements, but the temporal sequence is necessarily delayed and extended due

to the slower onset and polysynaptic nature of the imaged mitochondrial flavoproteins, which somewhat tempers direct comparisons of wave velocity across studies [17, 25].

Similarly, the determination of functional connectivity in this tangential slice preparation is constrained by the limitations of the LSPS mapping method [20, 33]. Although no functional long-range connections were observed in the slice, it remains possible that such connections are anatomically intact, but weak or silent to photostimulation [34, 35]. Whether such potentially weak, long-range connections are present and relevant to the propagation of cortical wave activity remains to be determined. Interestingly though, long-latency, presumably polysynaptic responses were easily elicited in the slice preparation, even at low stimulation intensities, suggesting that the maintained cortical circuit elements are predisposed to eliciting the polysynaptic responses necessary for propagating wave activity.

Despite their prevalence, the functional role of propagating wave activity remains unresolved, with potential influences ranging from developmental to computational [3, 7, 30, 36]. The occurrence of cortical waves across spatial and temporal scales may reflect an emergent phenomenon of the underlying connectional architecture, which has been appropriated to support these diverse roles [7, 12, 30]. A broader assessment of these potential functions may now be further enabled with the novel tangential cortical slice preparation described here.

Acknowledgements

We thank S. Ring for assistance with histological processing of specimens. This work was supported by NSF grant IOS1652342, and NIH grants R03NS109682 and R03AG056956.

FIGURE LEGENDS

Figure 1. Cytoarchitectural characterization of the tangential cortical slice preparation using a VGAT-Venus transgenic mouse strain. **A:** DIC image of the live tangential cortical slice preparation used for flavorprotein autofluorescence imaging. The sectioned is anchored at the edges with thin fibers connected to a metal harp. The stimulating electrode is positioned in the center of the slice (red star). Orientation axes: C, caudal; L, lateral. **B:** Organization of inhibitory VGAT-Venus positive neurons (green) in the tangential cortical slice. **C:** Phalloidin staining (red) of the tangential cortical slice preparation. Inset in *C* denotes the tangential slicing angle through the center of the slice preparation in the dorsal cerebrum (modified from Franklin and Paxinos, 2001). **D:** Cytoarchitecture of the slice preparation assessed using DAPI staining (blue).

Figure 2. Flavoprotein autofluorescence imaging of widespread activation in the tangential cortical slice preparation. **A:** Electrical stimulation of the slice (red star) results in multiple loci of divergent activation. FA image ($\Delta F/F$) is depicted at the time point of maximal activation. **B:** Percent of maximal ($\Delta F/F$) plotted as a function of time for the regions of interest indicated by the boxes in panel A. See also Supplementary Video 1. **C:** Example of electrical stimulation (red star) resulting in convergent activation towards the stimulating electrode. **D:** Plot of maximal ($\Delta F/F$) for the regions of interest in panel C. See also Supplementary Video 2.

Figure 3. Local functional connectivity in the tangential cortical slice assessed by laser-scanning photostimulation via glutamate uncaging. **A:** Whole-cell patch clamp recordings in voltage-clamp mode from a neuron in the barrel cortex of the tangential slice (red star) using a Cs+-intracellular solution to hold the neuron at depolarized potentials (-20 mV). Plot illustrates the recorded postsynaptic currents (PSCs) from stimulation at the site of overlay. Upward deflections indicate IPSCs and the downward deflections indicate EPSCs. **B-C:** Plots of the mean evoked currents at the stimulation sites from two cases. The plot is panel B is from the recordings in panel A.

REFERENCES

1. Naoumenko D, Gong P. Complex dynamics of propagating waves in a two-dimensional neural field. Front Comput Neurosci 2019; 13:50.
2. Gu Y, Qi Y, Gong P. Rich-club connectivity, diverse population coupling, and dynamical activity patterns emerging from local cortical circuits. PLoS Biol 2019; 15:e1006902.
3. Keane A, Gong P. Propagating waves can explain irregular neural dynamics. J Neurosci 2015; 35:1591-1605.
4. Hama N, Kawai M, Ito S, Hirota A. Optical study of interactions among propagation waves of neural excitation in the rat somatosensory cortex evoked by forelimb and hindlimb stimuli. J Neurophysiol 2018; 119:1934-1946.
5. Kang M, Lee YB, Gohel B, Yoo K, Lee P, Chung J, et al. Momentary level of slow default mode network activity is associated with distinct propagation and connectivity patterns in the anesthetized mouse cortex. J Neurophysiol 2018; 119:441-458.
6. Teramae JN, Fukai T. Local cortical circuit model inferred from power-law distributed neuronal avalanches. J Comput Neurosci 2007; 22:301-312.
7. Wu JY, Huang X, Zhang C. Propagating waves of activity in the neocortex: what they are, what they do. Neuroscientist 2008; 14:487–502.
8. Metherate R, Cruikshank SJ. Thalamocortical inputs trigger a propagating envelope of gamma-band activity in auditory cortex in vitro. Exp Brain Res 1999; 126:160-174.
9. Roland PE, Hanazawa A, Undeman C, Eriksson D, Tompa T, Nakamura H, et al. Cortical feedback depolarization waves: a mechanism of top-down influence on early visual areas. Proc Natl Acad Sci USA 2006; 103:12586–12591.
10. Song WJ, Kawaguchi H, Totoki S, Inoue Y, Katura T, Maeda S, et al. Cortical intrinsic circuits can support activity propagation through an isofrequency strip of the guinea pig primary auditory cortex. . Cereb Cortex 2006; 16:718–729.
11. Lu Y, Sato Y, Amari S. Traveling bumps and their collisions in a two-dimensional neural field. Neural Comput 2011; 23:1248-1260.
12. van Drongelen W, Lee HC, Stevens RL, Hereld M. Propagation of seizure-like activity in a model of neocortex. J Clin Neurophysiol 2007; 24:182-188.
13. Huang X, Xu W, Liang J, Takagaki K, Gao X, Wu JY. Spiral wave dynamics in neocortex. Neuron 2010; 68:978-990.
14. Huang X, Troy WC, Yang Q, Ma H, Laing CR, Schiff SJ, et al. Spiral waves in disinhibited mammalian neocortex. J Neurosci 2004; 24:9897-9902.
15. Franklin KBJ, Paxinos G. The mouse brain in stereotaxic coordinates. 2nd ed. New York: Academic Press; 2001.
16. Watkins PV, Kao JP, Kanold PO. Spatial pattern of intra-laminar connectivity in supragranular mouse auditory cortex. Front Neural Circuits 2014; 8:15.
17. Shibuki K, Hishida R, Murakami H, Kudoh M, Kawaguchi T, Watanabe M, et al. Dynamic imaging of somatosensory cortical activity in the rat visualized by flavoprotein autofluorescence. J Physiol 2003; 549(Pt 3):919-927.
18. Husson TR, Mallik AK, Zhang JX, Issa NP. Functional imaging of primary visual cortex using flavoprotein autofluorescence. J Neurosci 2207; 27:8665-8675.
19. Theyel BB, Lee CC, Sherman SM. Specific and nonspecific thalamocortical connectivity in the auditory and somatosensory thalamocortical slices. Neuroreport 2010; 21:861-864.

20. Shepherd GM. Circuit mapping by ultraviolet uncaging of glutamate. Cold Spring Harb Protoc 2012; 2012:998-1004.
21. Lee CC, Imaizumi K. Functional convergence of thalamic and intinsic inputs in cortical layers 4 and 6. Neurophysiol 2013; 45:396-406.
22. Lee CC, Sherman SM. Topography and physiology of ascending streams in the auditory tectothalamic pathway. Proc Natl Acad Sci U S A 2010; 107:372-377.
23. Suter BA, O'Connor T, Iyer V, Petreanu LT, Hooks BM, Kiritani T, et al. Ephus: multipurpose data acquisition software for neuroscience experiments. Front Neural Circuits 2010; 4:100.
24. Llano DA, Theyel BB, Mallik AK, Sherman SM, Issa NP. Rapid and sensitive mapping of long-range connections in vitro using flavoprotein autofluorescence imaging combined with laser photostimulation. J Neurophysiol 2009; 101:3325-3340.
25. Theyel BB, Llano DA, Issa NP, Mallik AK, Sherman SM. In vitro imaging using laser photostimulation with flavoprotein autofluorescence. Nat Protoc 2011; 6:502-508.
26. Wang Y, Kakizaki T, Sakagami H, Saito K, Ebihara S, Kato M, et al. Fluorescent labeling of both GABAergic and glycinergic neurons in vesicular GABA transporter (VGAT)–Venus transgenic mouse. Neuroscience 2009; 164:1031-1043.
27. Lee CC, Yanagawa Y, Imaizumi K. Commissural functional topography of the inferior colliculus assessed in vitro. Hear Res 2015; 328:94-101.
28. Lee CC, Yanagawa Y, Imaizumi K. Nicotinic alteration of functional thalamocortical topography. Neuroreport 2015; 26:688-694.
29. Namiki S, Norimoto H, Kobayashi C, Nakatani K, Matsuki N, Ikegaya Y. Layer III neurons control synchronized waves in the immature cerebral cortex. J Neurosci 2013; 33:987-1001.
30. Muller L, Chavane F, Reynolds J, Sejnowski TJ. Cortical travelling waves: mechanisms and computational principles. Nat Rev Neurosci 2018; 19:255-268.
31. Xiao Y, Huang XY, Van Wert S, Barreto E, Wu JY, Gluckman BJ, et al. The role of inhibition in oscillatory wave dynamics in the cortex. Eur J Neurosci 2012; 2012:2201-2212.
32. Husson TR, Issa NP. Functional Imaging with Mitochondrial Flavoprotein Autofluorescence: Theory, Practice, and Applications. In: Frostig RD, editor. In Vivo Optical Imaging of Brain Function 2nd edition. Boca Raton: CRC Press; 2009.
33. Imaizumi K, Yanagawa Y, Feng G, Lee CC. Functional topography and development of inhibitory reticulothalamic barreloid projections. Front Neuroanat 2018; 12:87.
34. Rumpel S, Hatt H, Gottmann K. Silent synapses in the developing rat visual cortex: evidence for postsynaptic expression of synaptic plasticity. J Neurosci 1998; 18:8863-8874.
35. Voigt T, Opitz B, de Lima AD. Activation of early silent synapses by spontaneous synchronous network activity limits the range of neocortical connections. J Neurosci 2005; 25:4605-4615.
36. Roberts JA, Gollo LL, Abeysuriya RG, Roberts G, Mitchell PB, Woolrich MW, et al. Metastable brain waves. Nat Commun 2019; 5:1056.

Figure 1

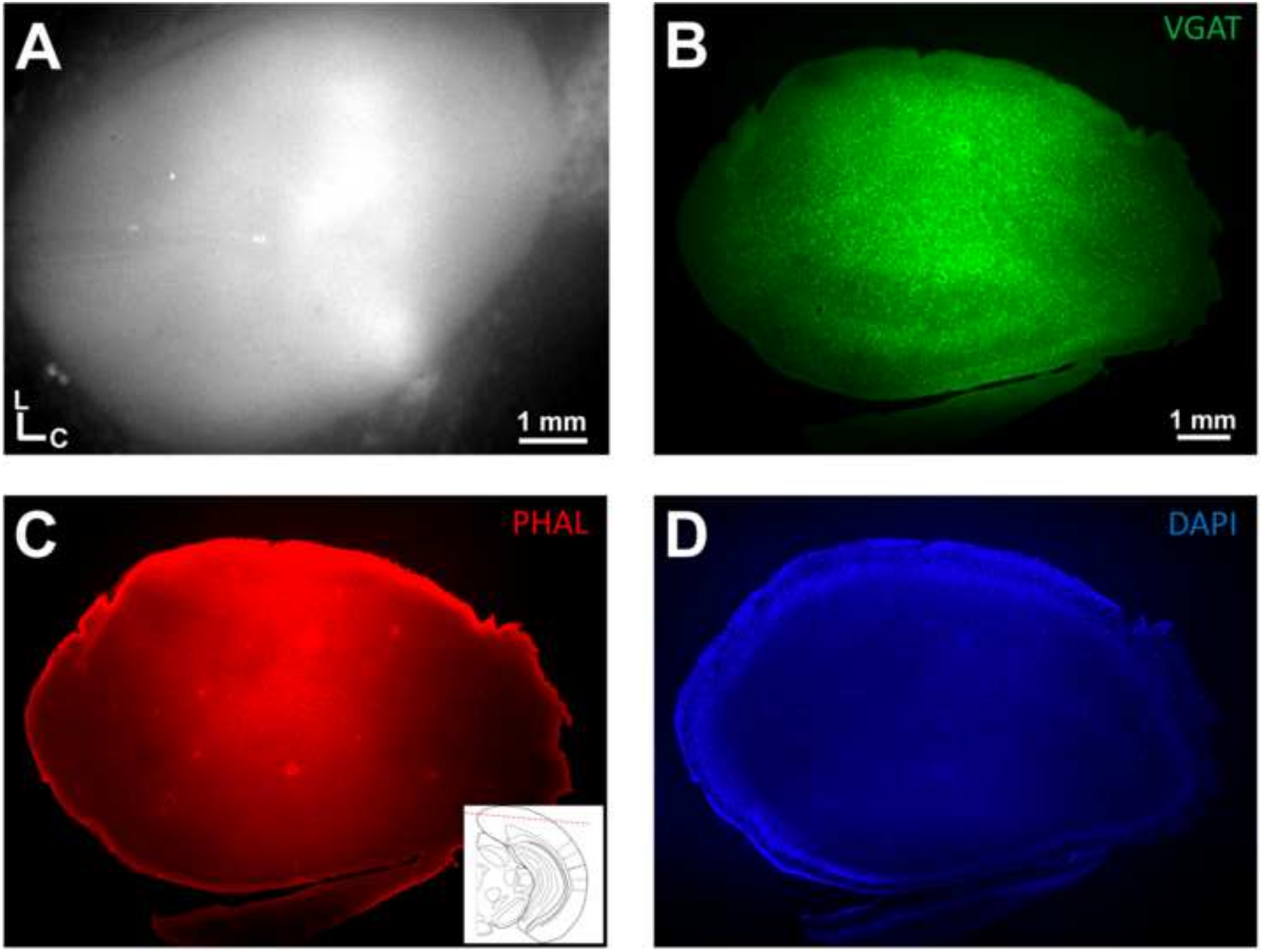

Figure 2

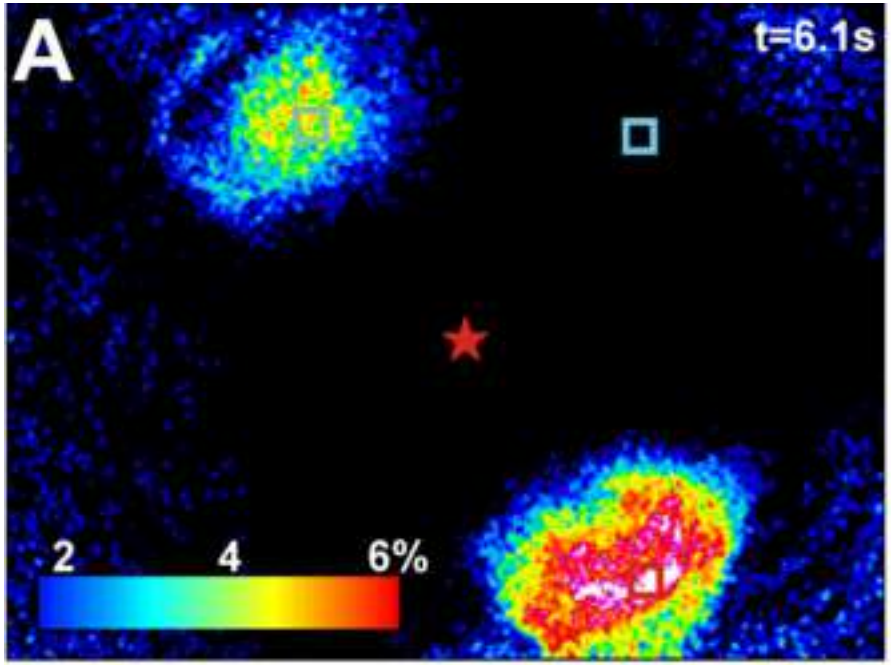

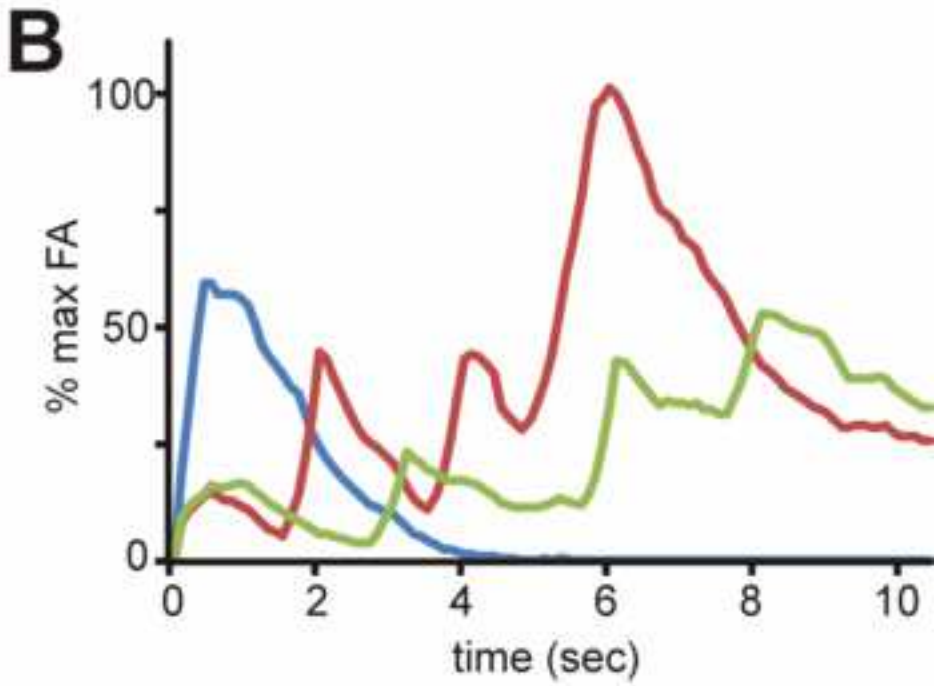

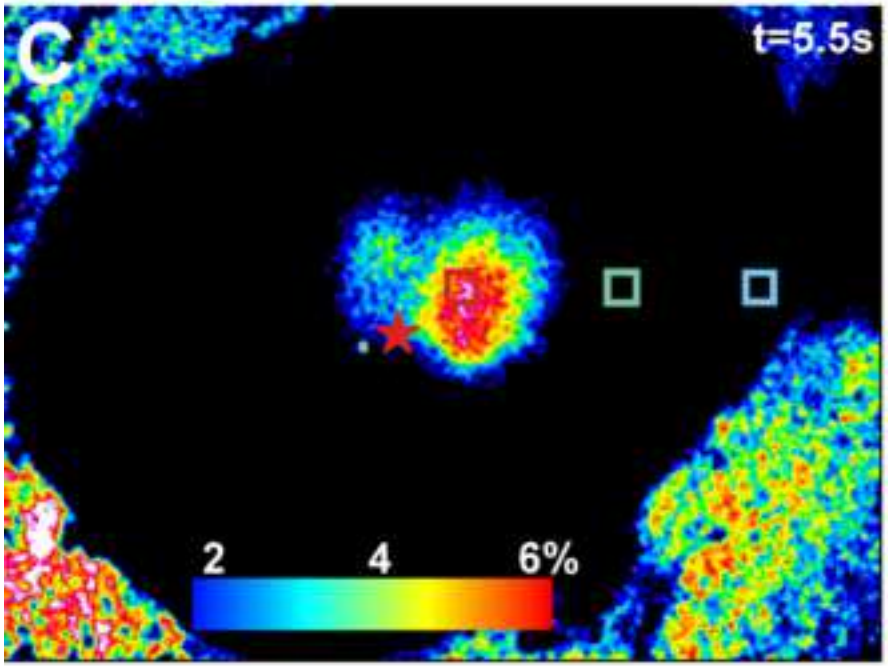

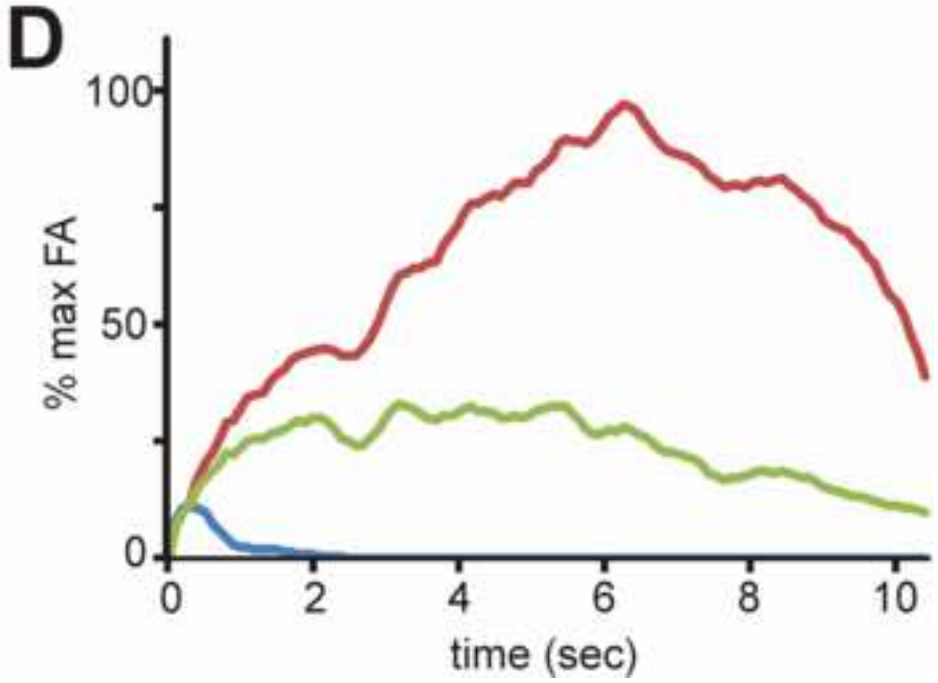

Figure 3